USE OF MICROFLUIDIC SYSTEMS FOR ASSEMBLY OF NUCLEIC ACID NANOPARTICLES

by
Marcos Manuel Pérez Millán

A thesis submitted to Johns Hopkins University in conformity with the requirements for

the degree of Master of Science in Engineering

Baltimore, Maryland
May 2022

ABSTRACT

Nucleic acid nanoparticles are effective in treating numerous diseases. Ionic complexes with polymers are used to facilitate the transport of nucleic acids, such as DNA, to intracellular target sites. Nanoparticles can be prepared manually with pipettes by mixing polyanionic acids and polycations. However, parameters like size, internal structure, and polydispersity of the complexes affect efficiency for pharmaceutical purposes. Therefore, a controlled assembly like microfluidics is important to maximize product quality [1]. Thus, the use of the NanoAssemblr Spark microfluidic system is explored in this project.

The use of lipid nanoparticles (LNPs) for nucleic acid delivery has gained attention in recent years as vaccine candidates or to treat diseases [2]. At AstraZeneca's Christie's group, peptide is also researched as a nucleic acid delivery technology, and the combination of peptide with the components of lipid nanoparticles is desired to be studied. The beginning phase of the project consisted of the fabrication of simple nanoparticles with peptide and green fluorescent protein (GFP) DNA. The second phase of the project consisted of fabricating hybrid nanoparticles (hNPs) with parameters chosen from the beginning phase. Hybrid nanoparticles consisted of lipid, peptide, and GFP-DNA. Also, a numerical simulation was developed to understand the mixing characteristics of the microfluidic system.

Some key findings from this project were that hybrid nanoparticles assembled by microfluidics were smaller in size and polydispersity (or were more uniform) than by pipetting, leading to higher desirability. In addition, the optimal concentration of lipid in the hybrid nanoparticles was found to be 0.6 mg/mL. Lastly, peptide-only nanoparticles enabled more DNA expression than hybrid nanoparticles and were generally of smaller size.

From the numerical simulation, it was discovered that depending on the solutions' concentrations, flow rate ratios of 2:1 or 3:1 (nucleic acid to organic solution) are optimal for mixing quality which can be further improved by having a smaller total flow rate.

In conclusion, it is recommended to continue exploring microfluidics for assembling hybrid nanoparticles. However, a system with more flexibility is recommended, such as one where the flow rate ratio and total flow rate can be controlled.

Primary Reader and Advisor: Soojung Claire Hur

Secondary Reader: Gretar Tryggvason

ACKNOWLEDGEMENTS

From the Johns Hopkins University, I wish to express my gratitude to Assistant Professor Claire Hur and her students, and Professor Gretar Tryggvason. From AstraZeneca, I wish to express my gratitude to Principal Scientist Ronald James Christie, Senior Scientists Hannah Vaughan and Morgan Urello, Scientist Chacko Chakiath, and Associate Scientist Lucia Xiang. Thank you all for your patient teaching and guidance during my project.

DEDICATION

In loving memory of Agustin Millán. Thank you for your wisdom and your rich, never-ending true love.

Psalm 27:1.

CONTENTS

List of Tables

List of Figures

Chapter 1

INTRODUCTION

1.1 Motivation:

Microfluidic devices have a wide range of biological and chemical applications. These include uses in medical diagnostics, drug development, and DNA and protein analysis. Microfluidic devices can be made in miniature sizes which allows for rapid analysis using portable instruments. Also, they can consume few reagents and use minimal amounts of samples, which reduces waste and can lead to low-cost operations [3].

At AstraZeneca's Christie's group, nanoparticles were traditionally prepared manually with the use of pipettes. The NanoAssemblr Spark microfluidic system was chosen to be explored, as it enables the fast, intuitive, and easy ultra-low volume production of nanoparticles [4]. With the Spark, there are more controlled mixing conditions, and it is reproducible, which can result in nanoparticles that are smaller in size with lower polydispersity. Also, due to the Spark's electronic control that allows researchers to select the pressurizing setting (depending on the volume of material being used), batch-to-batch and user variability can be minimized. However, the Spark was optimized for lipid nanoparticles only, whereas Christie's team is interested in making nanoparticles composed of peptide, and peptide with lipid and cholesterol. Therefore, the Spark requires troubleshooting and testing to determine what works best for the team's needs.

1.2 Review:

Lipid nanoparticles have various components, including structural lipid, cholesterol, cationic/ionizable lipid, PEG-lipid [2], and in the case of hybrid nanoparticles, peptide. Therefore, successfully assembling them requires different methods other than mixing by pipetting. This was

confirmed in the laboratory, as hybrid nanoparticles containing lipid and peptide were assembled by pipetting and the use of the vortex mixer, which agitates fluid samples with vortex generation. Their dynamic light scattering (DLS) data showed high-sized nanoparticles (larger than 250 nm) that are not desirable for nucleic acid delivery. This is further discussed in section 3.2 of Results and Discussion and is shown in Figure 3.7.

Traditionally, lipid nanoparticle–nucleic acid formulations were made by reverse-phase evaporation, thin-film hydration, or other methods. Then, the nanoparticle sizes were further homogenized by different extrusion techniques. Currently, lipid nanoparticle formulations are generally manufactured by rapid mixing with the use of microfluidics [5].

In contrast to conventional lipid nanoparticle production methods, microfluidics offers a more reproducible manufacturing method, controlled manufacturing conditions that result in homogenous nanoparticle formation, high nucleic acid loading efficiency in a one-step formulation process, fast production and optimization, and a path to scaling up production [6].

The Spark instrument operates using a pressure-driven mechanism, exerting the same pressure on both input wells of the Spark cartridge for mixing of the materials [4]. The following figure is an image of the cartridge. The mixing of the fluids occurs in the toroidal zone of the microchannel:

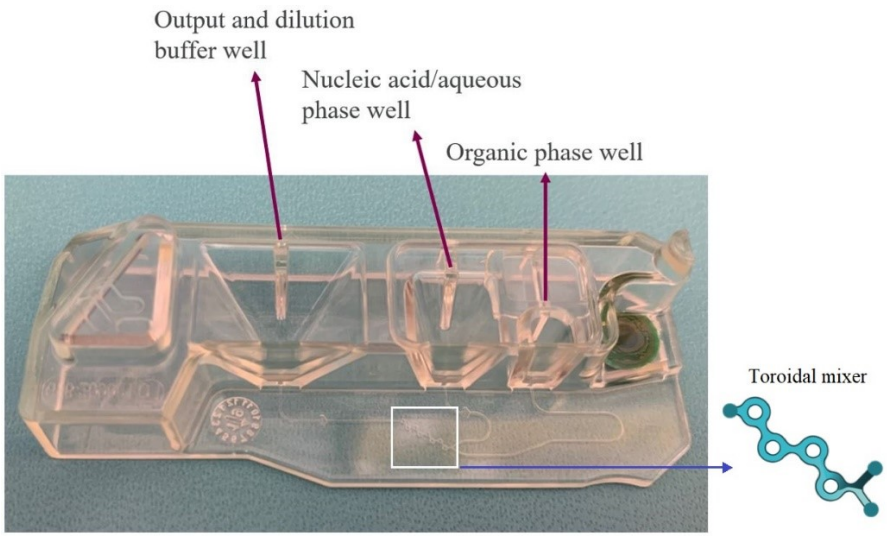

Figure 1.1: NanoAssemblr Spark cartridge. For the flow to begin, pressure is applied on the right-most two wells, which are the input wells. The aqueous phase well holds double the volume of the organic phase well

One pipettes the nucleic acid and organic materials in their respective wells, loads the cartridge in the Spark, selects a pressure setting, and runs the machine. In a few seconds, the cartridge can be removed, and the nanoparticles can be pipetted out from the output well. The following image is a visual representation of the mixing in the microchannel (left). The resultant nanoparticles are then ready for transfection in cells (right):

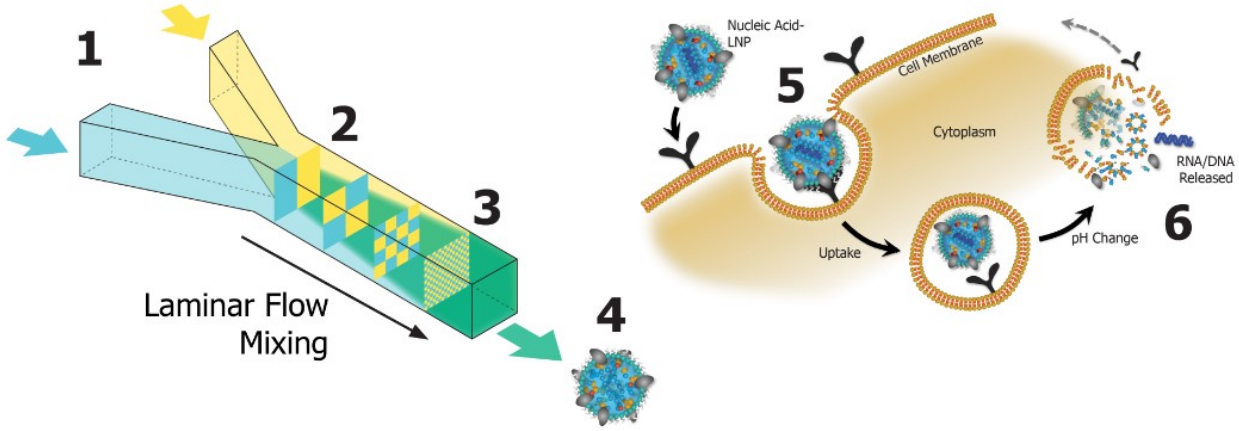

Figure 1.2: Mixing in the microchannel and transfection visual representations [6]

Various parameters of the NanoAssemblr Spark and nanoparticle formation were studied during this project. Those were the following:

Pressure settings: The pressure settings vary from 1 through 9, and they are selected depending on the volume of nanoparticles desired to be produced. The lowest setting is for the smallest volume, and vice-versa. The settings do not specify the exact amount of pressure applied.

Order of the wells: As seen in Figure 1.2 above, the aqueous and organic phases have designated wells. As it is shown there, the setup is denoted as the "traditional order of the wells." In the traditional order of the wells, the aqueous phase well is to have double the volume of the organic phase, and the dilution buffer well is to have a volume equal to the sum of the organic and aqueous phase wells. Now, this order can be switched, and one would load the organic phase in the aqueous phase well, and vice-versa. This setup is denoted as "switched wells," where the organic phase is to have double the volume of the aqueous phase, with the dilution buffer well still having a volume equal to the sum of the other two wells.

N:P ratio: This is the ratio of positively-chargeable polymer amine (N = nitrogen) groups from the peptide, to negatively-charged nucleic acid phosphate (P) groups [4].

Parameters such as flow rate ratio (FRR) and total flow rate (TFR) cannot be manually selected in the Spark. The total flow rate is set at 200 mL/min [7], while the flow rate ratio stays constant at 2:1 (larger input well to smaller well).

1.3 Objectives and Scope:

The overall objective of this project can be summarized as the study of the mechanics of microfluidics and its effect on the biology of cells.

- 1st objective: To assemble peptide-only nanoparticles with microfluidics and manually (by pipetting), and to characterize by DLS and evaluate them via transfection *in vitro* (outside of the living body and in an artificial environment)
    - Determine the optimal N:P ratio, pressure setting, and Spark cartridge well order
- 2nd objective: To research hybrid nanoparticles by microfluidics with the optimal settings from the 1st objective
- 3rd objective: To numerically model and study the microfluidic mixing phenomenon that occurs in the NanoAssemblr Spark microfluidics system

Chapter 2

METHODOLOGY

2.1 Simulation:

A numerical simulation of the microchannel mixing was carried out with the use of the commercially available software COMSOL Multiphysics. To do so, it is required that one has the geometry of the microchannel mixer found in the NanoAssemblr Spark cartridge, which is shown in the following image:

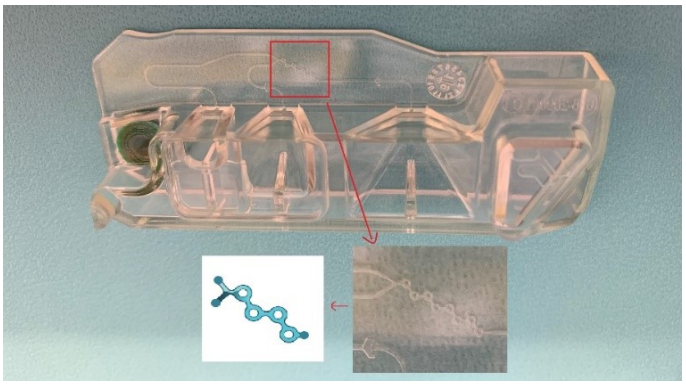

Figure 2.1: NanoAssemblr Spark cartridge geometry

The cartridge was observed under a microscope at the Assistant Professor Hur's laboratory, or the "Hur Lab for µFluidic Biophysics:"

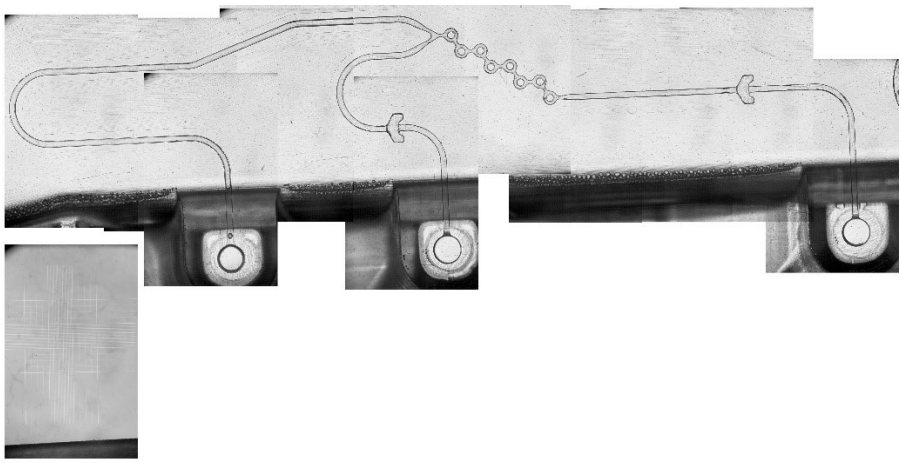

Figure 2.2: NanoAssemblr Spark cartridge microscope image (4x)

These images were measured using a MATLAB measure tool [8], and a CAD (computer-aided design) model of the geometry was built with the use of commercially available software SolidWorks. The following is a drawing exchange format (DXF) file of the geometry:

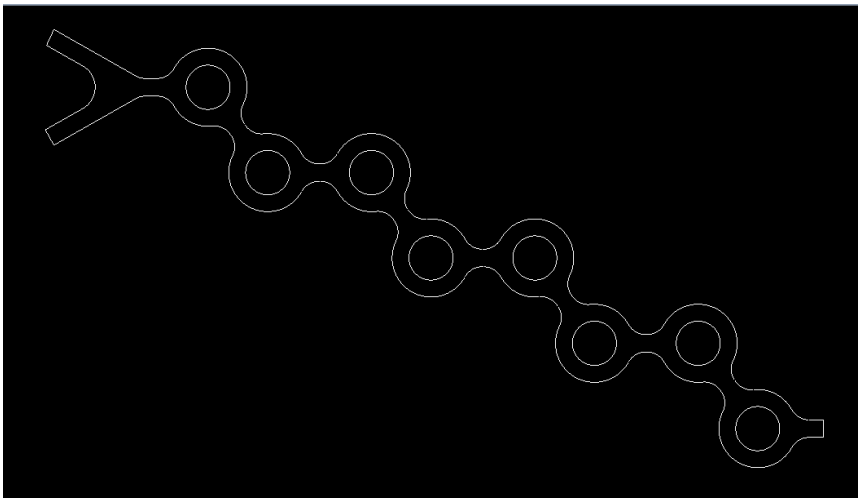

Figure 2.3: DXF image of the microchannel mixer. On the left-hand side, there are the two inlets, one for organic material (top), and the other for the aqueous phase (bottom)

Next, the geometry was imported into COMSOL for the simulation to take place. In COMSOL, the chosen physics interface was the transport of diluted species under laminar flow. The transport of diluted species interface can be used to calculate the concentration field of a dilute solute in a solvent. It can also model the transport and reactions of the species dissolved in a liquid, gas, or solid. The driving forces for transport can be diffusion by Fick's law, convection when coupled to a flow field, and migration when coupled to an electric field [9]. For this project's simulation, the driving force is diffusion by Fick's law and convection is the transport mechanism. The diffusion coefficient for both species is set as the default of 1×10^{-9} m^2/s. Now, these were the chosen parameters in the numerical simulation:

Table 2.1: COMSOL parameters. Inlet 1 is the organic material and inlet 2 is the nucleic acid solution. These chosen parameters are changed in certain studies

Parameter	Description	Value	Unit
v_1	Inlet 1 normal inflow velocity (organic)	0.025	cm/s
v_2	Inlet 2 normal inflow velocity (nucleic acid)	0.05	cm/s
c_1	Inlet 1 concentration	20	mol/m^3
c_2	Inlet 2 concentration	10	mol/m^3

As seen above, the selected concentration values are arbitrary. This is because the simulation solves the convection-diffusion equation, where the concentration value is a scalar. Also, the chosen materials were the following: water throughout the inside domain of the channels, air inside the domains of the inner walls (or circles), and polydimethylsiloxane (PDMS) for all walls or boundaries. Under laminar flow,

the outside boundaries of the channels were selected as walls, and the inside boundaries (or circles) were selected as interior walls.

Now, a grid study was done to determine the proper grid or mesh, which is a physics-controlled mesh, and the extra-fine mesh was chosen (see Appendices – 5.1.1 Grid Study). Also, a time step study was done, and it was determined that the time step chosen did not influence the simulation's results. This means that the software uses an implicit solution method, which allows for large time-step sizes. Thus, the time step used is 25 seconds. See Appendices – 5.1.2 Time Step Study for an explanation of the study and the time scale of the simulation.

To analyze the mixing quality of the solutions at the outlet of the toroidal mixer, it is useful to determine the width of the mixed region, which refers to the width in the mixer where the organic and nucleic acid solutions have equal (or overlapping) concentrations. A larger width of the mixed region means that the solutions have mixed more thoroughly, and vice-versa. This was done by plotting the minimum of the two concentrations bounded by a limit of detection, greater than 4 mol/m^3.

The width of the mixed region is evaluated across the length of the outlet of the channel. In COMSOL, this can be done through a linear projection, which allows one to integrate the expression of the mixed region (minimum of the two concentrations bounded by the limit of detection) along a one-dimensional path by mapping the two-dimensional channel space into a one-dimensional line. The selected domain is the inside of the channels, and an origin and an *x* component are selected, along which the line that is integrated will stretch. The following image shows the cut line through the center of the outlet, across which it is desired to know the mixed region width:

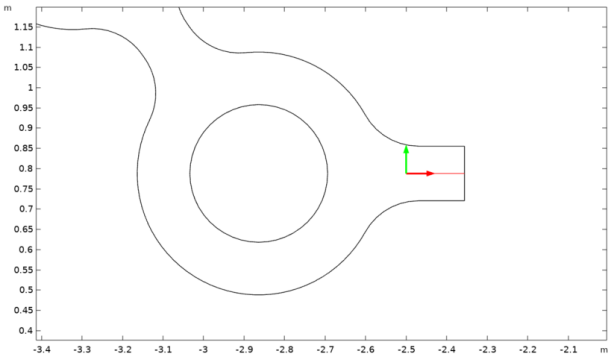

Figure 2.4: Cutline for determining the width of the mixed region

Also, a one-dimensional plot group line graph is added with the data set of the cutline, and with the expression of the linear projection (the minimum of the two concentrations above the limit of detection). This expression is divided by a strictly true condition to normalize it. Thus, the normalized width of the mixed region is plotted as a function of length [10].

2.2 AstraZeneca Experiments:

Various experiments were carried out in the Biologics Engineering laboratory at AstraZeneca. Nanoparticles were assembled with the use of the NanoAssemblr Spark or manually, by pipetting. The nanoparticles were characterized by dynamic light scattering (DLS) (see Appendices – 5.1.3 Dynamic Light Scattering). DLS allows one to determine the size, polydispersity (or uniformity), and count rate of the nanoparticles, which help to determine the number of nanoparticles that were assembled.

The function of the nanoparticles was determined *in vitro* through transfection with H1299 cells, and their DNA expression was studied through quantitative live-cell imaging and analysis with the use of the Incucyte (see Appendices – 5.1.4 Incucyte). Also, the DNA encapsulation efficiency was determined with the use of gel electrophoresis (see Appendices – 5.1.5 Gel Electrophoresis).

First, peptide-only nanoparticles were explored. During this phase of the experiment, the NanoAssemblr Spark pressure setting, order of the wells, and N:P ratios were tested. Then, peptide and lipid nanoparticles were studied, which can be referred to as hybrid nanoparticles. During this second phase of the experiment, different concentrations of lipid were explored based on suggestions from literature [2].

Chapter 3

RESULTS & DISCUSSION

3.1 Simulation:

3.1.1 Inlet Velocity Study:

An inlet velocity study was conducted to determine the effect of lowering the total flow rate on the mixing quality at the outlet of the mixer. This was done for the case in which both solutions are at the same concentration, and the flow rate ratio is locked at 2:1. It was found that as the total flow rate decreases, the mixing quality at the outlet of the mixer is better, which equates to nanoparticles of better quality (see Appendices – 5.1.6 Inlet Velocity Study).

From literature [2], a lower total flow rate ratio in the toroidal mixer produced smaller-sized nanoparticles (around 5 nm smaller) with a smaller polydispersity. This supports the findings from the inlet velocity study.

3.1.2 Parametric Sweeps on Inlet 2's Velocity (v_2), or the Ratio of Nucleic Acid Solution Velocity to Organic Solution Velocity (v_2/v_1):

Parametric sweeps were carried out to determine the effect of changing the flow rate ratio on the mixing quality at the outlet. The width of the mixed region was plotted along the cutline shown earlier (Figure 2.4):

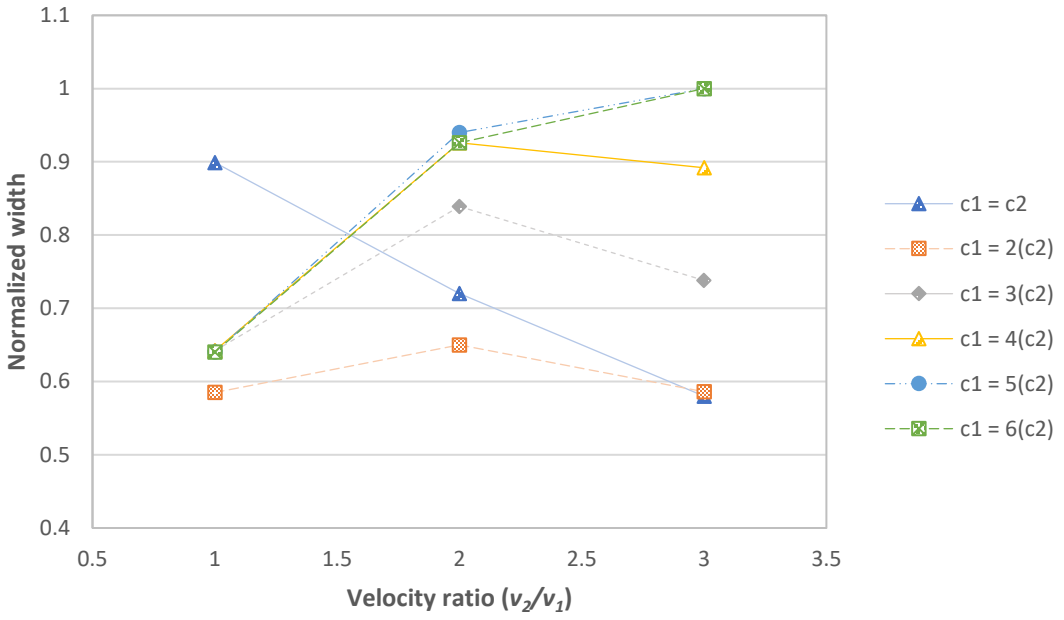

Figure 3.1: Normalized width of the mixed region for varying inlet concentration and flow rate ratios. A larger width of the mixed region means better mixing quality (c_2 stays constant at 10 mol/m^3)

As seen in the previous figure, when the solutions are at the same concentration, the optimal velocity or flow rate ratio is 1:1. However, different concentrations were also observed because in the physical system (with the traditional order of the wells), the organic solution is at a higher concentration. When the concentration of the organic solution is double that of the nucleic acid solution, the optimal flow rate ratio was 2:1. This was also the case when the concentration ratios were 3 and 4. Now, when the concentration ratios were 5 and 6, the optimal flow rate ratio was 3:1. In the physical experiments, the organic to nucleic acid solution ratios vary for different studies, so different flow rate ratios could be used to improve the quality of the nanoparticles. For the original figures from COMSOL, see Appendices – 5.1.7 Velocity Ratio Study.

3.2 AstraZeneca Experiments:

3.2.1 First Phase:

During the first phase of the project, the team worked with peptide-only nanoparticles to determine the best N:P ratio, Spark pressure setting, and order of the wells at which to assemble the nanoparticles.

First, a study was done to determine the optimal N:P ratio by testing ratios of 1, 2, and 4. The following plot shows the protein (GFP DNA) expression as analyzed with the use of the Incucyte, which can also be referred to as green area:

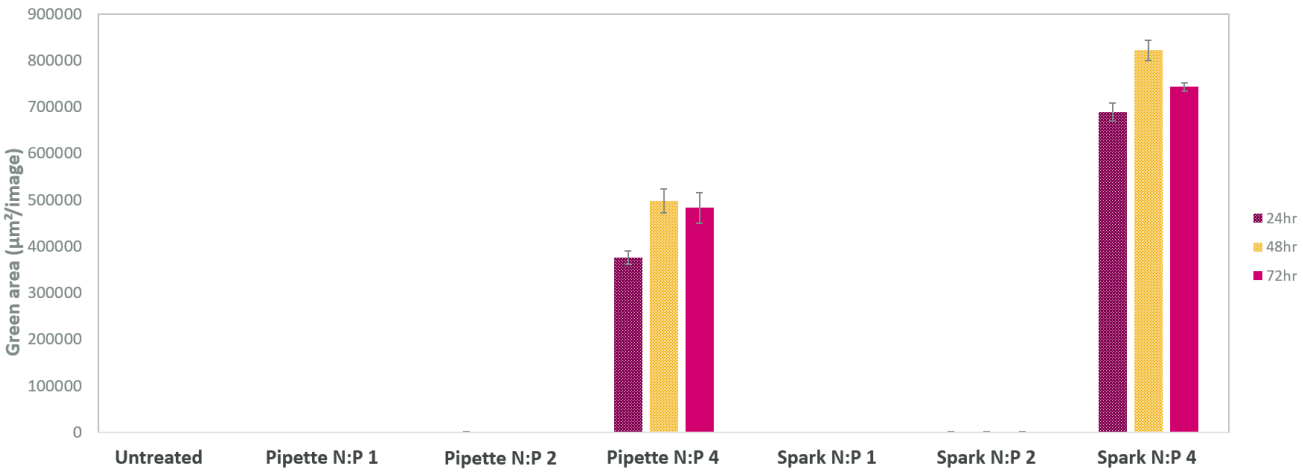

Figure 3.2: Protein expression for different N:P ratios. "Spark" refers to nanoparticles assembled with the NanoAssemblr Spark with the traditional order of the wells, and "Pipette" refers to nanoparticles assembled manually by pipetting

As seen, the N:P ratio of 4 significantly enabled more green area than ratios of 1 and 2, which were negligible in comparison and cannot be seen in the bar graph. Thus, the selected N:P ratio was that of 4.

Next, with the chosen N:P ratio of 4, the pressure settings and order of the wells were tested. The following plot shows the protein expression for various settings and with the order of the wells switched:

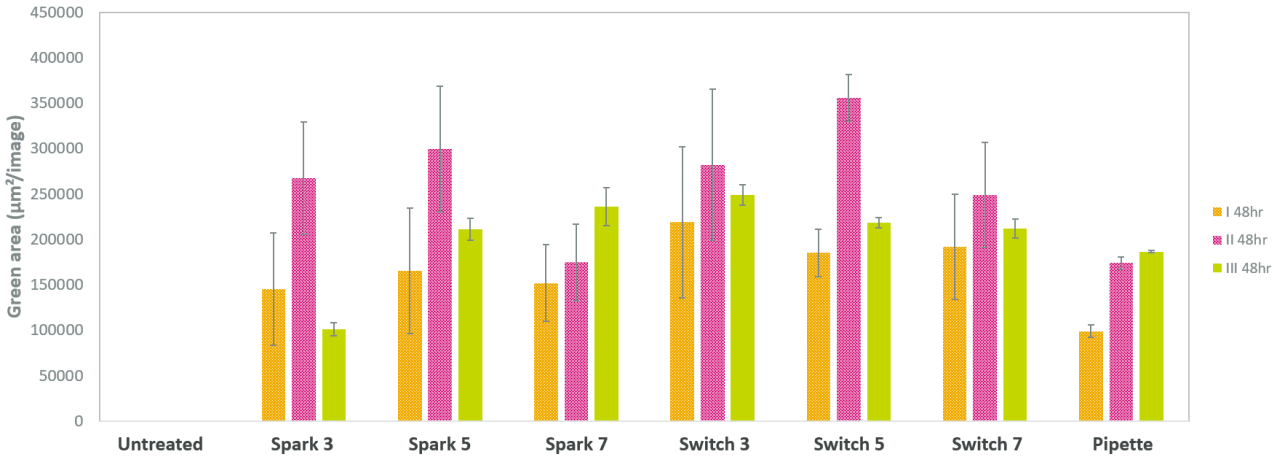

Figure 3.3: Protein expression for the different settings at 48 hours for three repeats of the experiment. "Switch" refers to nanoparticles assembled with the NanoAssemblr Spark but with the order of the wells switched

As seen, there was variation between the experiments and no clear trend on how the settings or the switching of the wells affect the DNA expression. Now, an additional test was done to strictly test the pressure settings. The following plot shows the green area for this experiment:

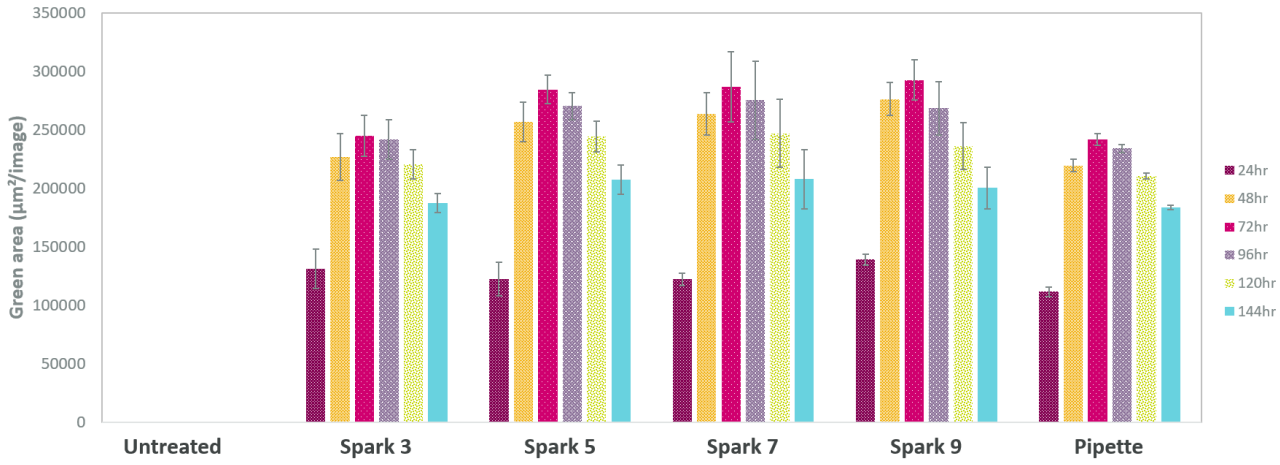

Figure 3.4: Protein expression for only the various pressure settings

As seen above, there is also not a clear difference in DNA expression between the various settings.

Additionally, it is useful to observe a comparison in DLS characterization for the various pressure settings and switching of the wells:

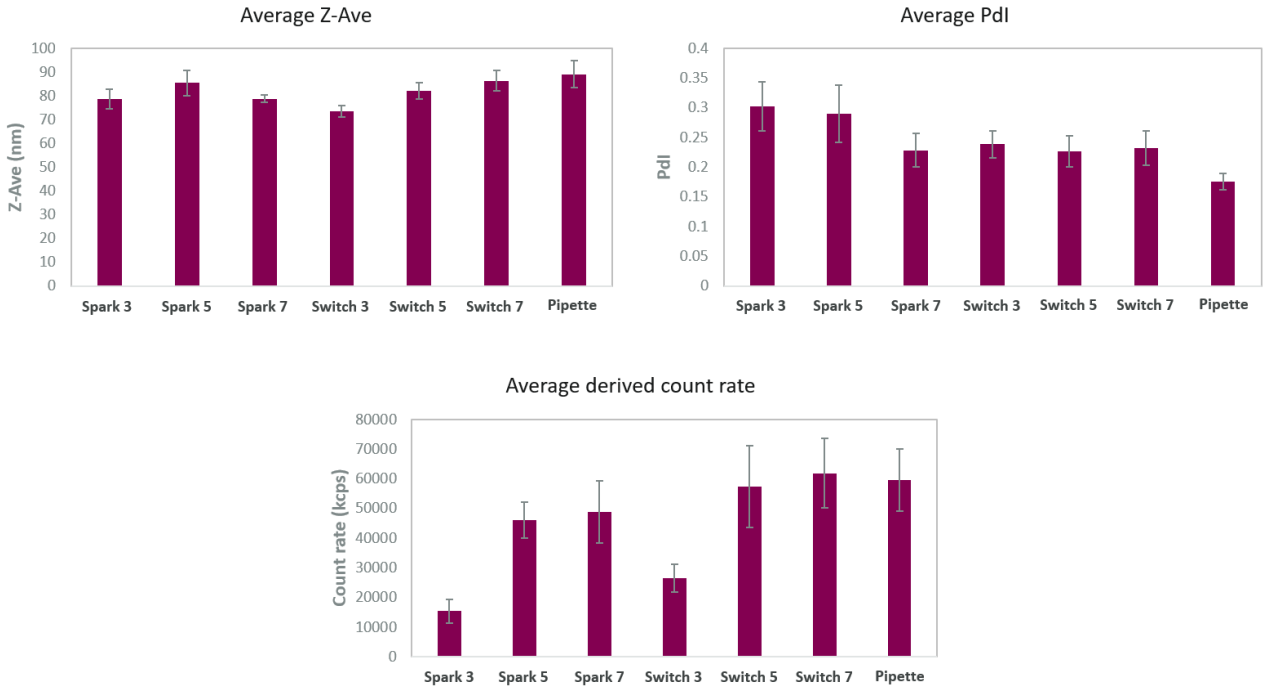

Figure 3.5: DLS data comparison. Averages for five experiments. Higher PdI means lower uniformity

As seen above, pipette nanoparticles were similar to Spark nanoparticles, just like in the DNA expression plots shown before. Also, one can see that setting 3 has a significantly smaller count rate. This is likely because there is less material for the lower pressure settings, so fewer nanoparticles are assembled during steady-state, when the output flow is as mixed as it can be. Therefore, if possible, this setting should be avoided.

Changing the pressure settings or switching the order of the wells did not have a significant impact on either DLS or transfection data. Therefore, the team selected setting 5, as it outputs the right amount of material needed for experiments with very little waste. Also, the traditional order should be used for hybrid nanoparticles, as for them, it is required to dissolve the organic material in ethyl alcohol. Due to ethyl alcohol's small surface tension, it can pre-maturely flow easily into the mixing channel before the NanoAssemblr Spark applies pressure on the wells. A way to overcome this issue is by loading the dilution buffer and organic wells first, which provide back pressure and in turn makes the pre-mature flow of ethyl alcohol less likely.

In summary, the selected settings for the next steps were Spark pressure setting 5, the traditional order of wells, and an N:P ratio of 4.

3.2.2 Second Phase:

For the second phase of the project, the team focused on hybrid nanoparticles which consist of organic material composed of lipid (DSPC), cholesterol, and peptide. While the nucleic acid solution was still GFP DNA. Together, DSPC lipid and cholesterol are referred to as simply "lipid." For these experiments, the concentrations of lipid were varied from a range of 4 mg/mL to 0.1 mg/mL based on suggestions from literature [2]. Using an N:P ratio of 4 and the previously selected settings, the DNA

concentration was kept constant and equal to previous experiments. The following figure shows the green area for the first experiment of this phase:

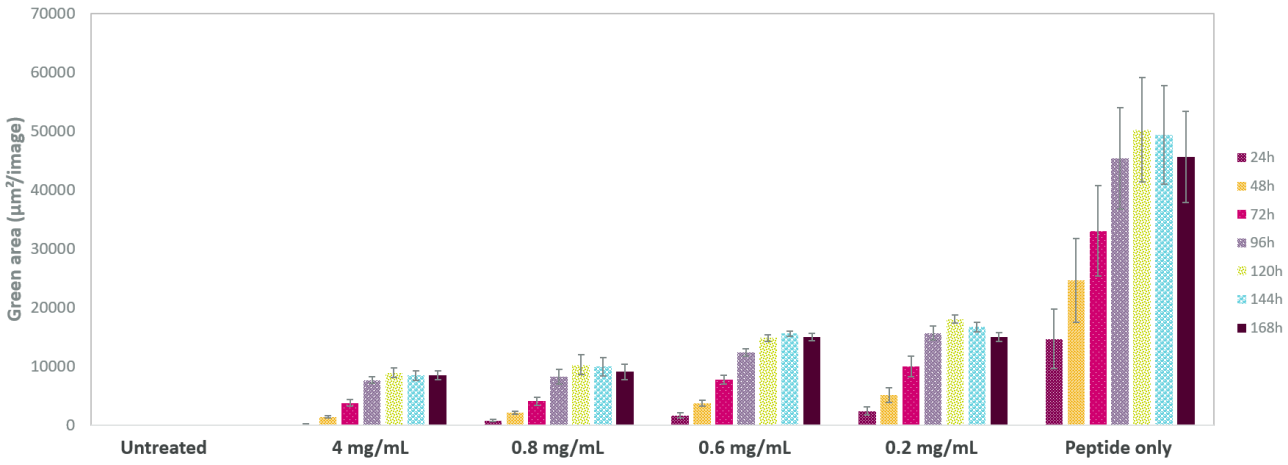

Figure 3.6: Protein expression for decreasing lipid concentrations and peptide-only nanoparticles

As seen above, peptide-only nanoparticles enable more DNA expression than hybrid nanoparticles. Also, for a smaller lipid concentration, the DNA expression is slightly more.

Next, it is necessary to observe the DLS characterization for all the studied hybrid nanoparticles with varying lipid concentrations:

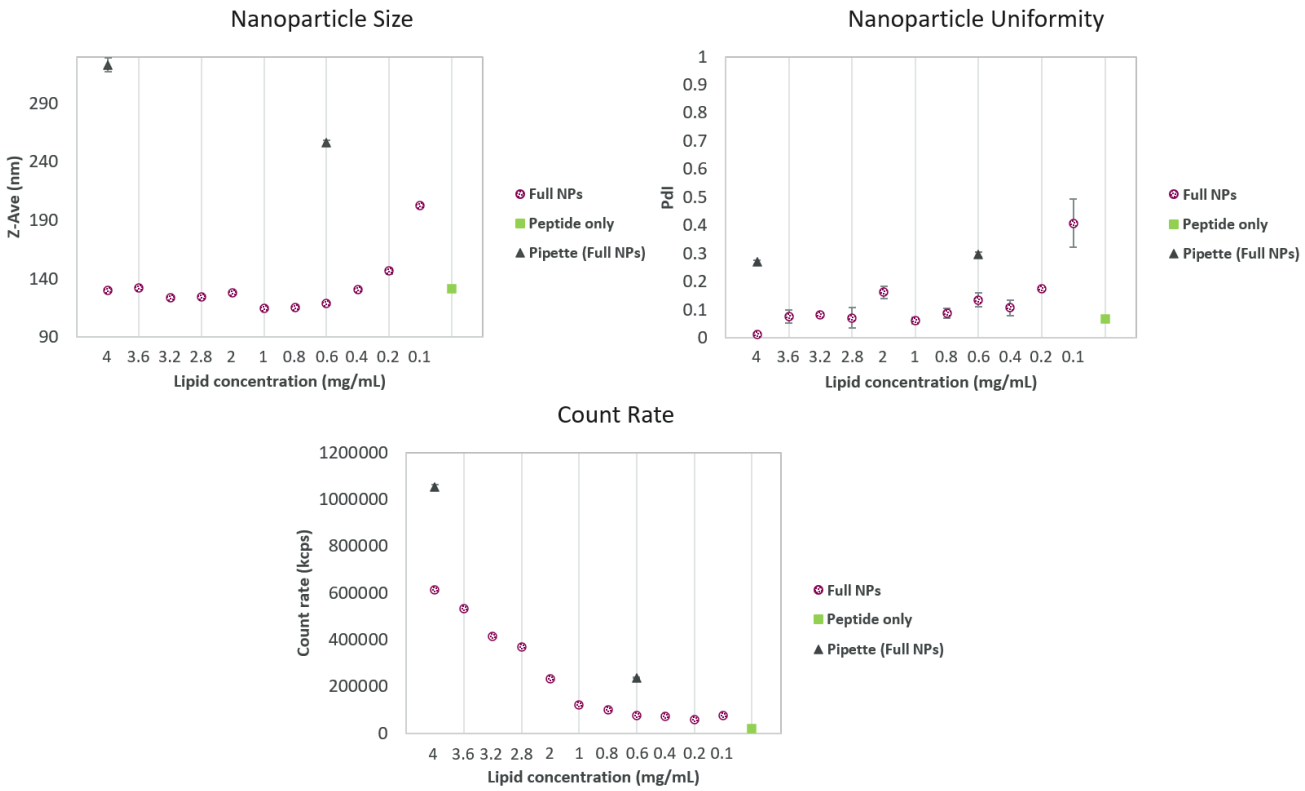

Figure 3.7: DLS data providing nanoparticle (NPs) size, uniformity, and count rate

As seen, the size of full hybrid nanoparticles stays relatively constant as the lipid concentration decreases from 4 mg/mL, but it begins to increase at low concentrations. Then, it returns to a smaller size with peptide-only nanoparticles, which is consistent with the first phase of the project. Also, the count rate decreases until about the concentration of 0.6 mg/mL and is nearly constant for smaller concentrations. From 0.6 mg/mL to 4 mg/mL, as the count rate goes up and the size stays constant, one can infer that there are either empty nanoparticles or nanoparticles with a smaller quantity of DNA, given that the DNA concentration during assembly is the same for all cases. This is supported by previous protein expression data (Figure 3.6), where smaller concentrations of lipid enabled more DNA expression. Therefore, the optimal lipid concentration for hybrid nanoparticles is 0.6 mg/mL, given that higher concentrations enable less green area, and smaller concentrations tend to make higher-sized

nanoparticles. However, it is worth noting that peptide-only nanoparticles enabled more DNA expression than hybrid ones and had desirable sizes too. Lastly, one can see that hybrid nanoparticles made by pipetting instead of with the NanoAssemblr Spark were much bigger in size and polydispersity, which reinforces the importance of using microfluidics to assemble properly sized lipid and hybrid nanoparticles.

Chapter 4

CONCLUSIONS AND FUTURE WORK

The NanoAssemblr Spark microfluidic system was studied as an assembling tool for peptide and peptide-lipid (hybrid) nanoparticles. With the results from the first phase of the project, it was concluded that nanoparticles are of similar characteristics and function with any of the Spark pressure settings. However, the smallest settings should be avoided due to the lower number of nanoparticles assembled. It was also concluded that switching the order of the wells did not affect the quality of the nanoparticles, so it was decided to use the traditional order of the wells. Lastly, it was seen that an N:P ratio of 4 enabled more *in vitro* DNA expression. During the second phase of the experiment, it was found that hybrid nanoparticles assembled by microfluidics were smaller in size and polydispersity than by pipetting. The optimal lipid concentration in the hybrid nanoparticles was found to be 0.6 mg/mL, as lower concentrations produced higher-sized nanoparticles, and higher concentrations enabled less DNA expression. However, peptide-only nanoparticles significantly enabled more DNA expression and had similar characteristics (but generally smaller) as hybrid nanoparticles with lipid concentrations of 0.6 mg/mL.

From the numerical simulation, it was found that a smaller total flow rate improved the mixing quality at the outlet of the microchannel mixer. Also, the flow rate ratio had a noticeable effect on the mixing quality as well, depending on the solutions' concentration ratios.

Future steps are to study further hybrid nanoparticles with different ionizable and structural lipids and peptides to make them more efficient at enabling DNA expression than peptide-only nanoparticles. In addition, it is suggested to use a microfluidic system with more flexibility than the NanoAssemblr Spark. During the mixing process, it would be advantageous to have control over the flow

rate ratio and the total flow rate. This flexibility would give freedom to researchers to tune the microfluidic system to assemble hybrid nanoparticles of the highest quality.

Chapter 5

REFERENCES

5.1 Appendices:

5.1.1 Grid Study:

A qualitative grid study was done for the various physics-controlled meshes in COMSOL:

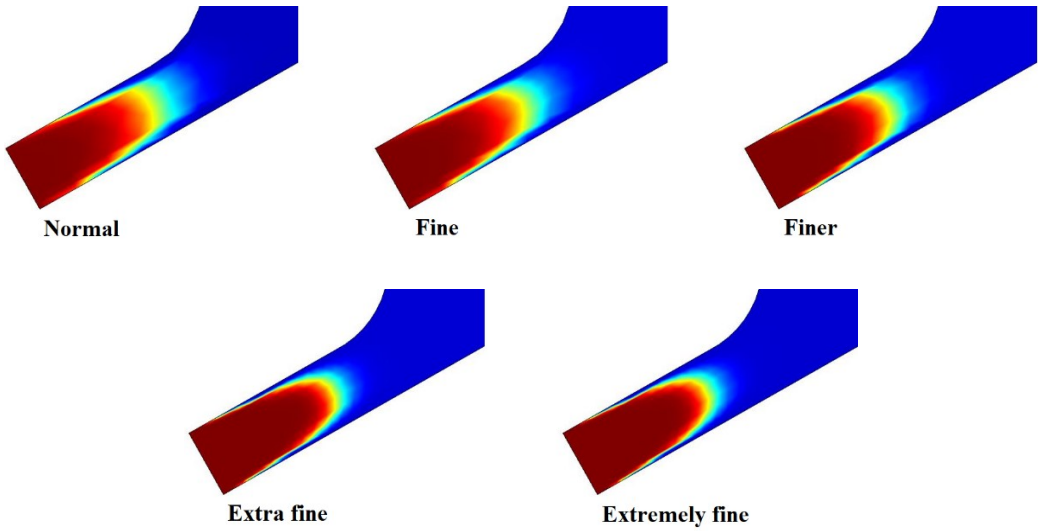

Figure 5.1: Qualitative grid study

As seen, the extra fine and extremely fine grids look quite similar. Also, a quantitative grid study was carried out by observing the width of the mixed region at the outlet for the extra fine and extremely fine grids:

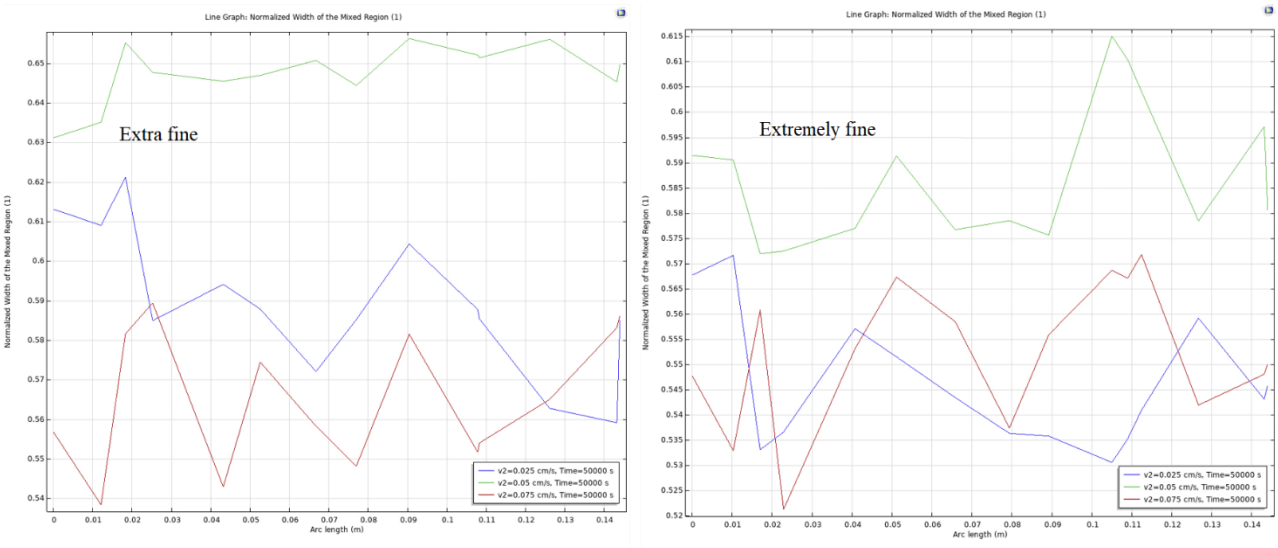

Figures 5.2 & 5.3: Quantitative grid study for extra fine (left) and extremely fine (right) grids

As seen, there is a small difference in mixed region width for the two grids. However, the trends are similar. Thus, the extra-fine grid was used in the simulation as it requires less computational power.

5.1.2 Time Step Study:

A time step study was done:

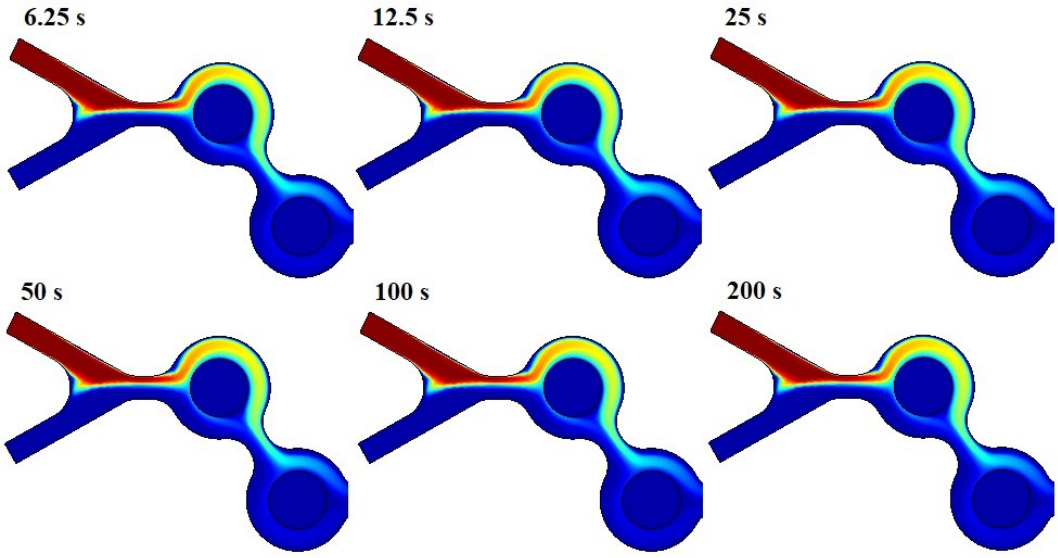

Figure 5.4: Time step study and plot of inlet 1's concentration at the same time

As seen above, the different time steps do not influence the concentration plots. Also, it is important to mention that the time scales in the simulation do not reflect the real system within the NanoAssemblr Spark, where the mixing occurs in about 10 seconds. However, since the simulation sought to answer questions during steady-state, such as the mixing quality, the time scale is not an issue.

5.1.3 Dynamic Light Scattering (DLS):

DLS allows for the measurement of the Brownian motion (or the random movement of particles due to collisions with solvent molecules) of particles in a dispersion and determines their hydrodynamic size using the Stokes-Einstein (SE) equation. The rate of the Brownian motion is quantified as the translational diffusion coefficient *D*, and the hydrodynamic size is the size of a sphere that diffuses at the same rate as the measured particles. Particles that are illuminated by a laser will scatter some of the light that hits them, and since they are in a dispersion, diffusion will cause the intensity of light scattered

by the particles to fluctuate over time. The detected light scattered from randomly diffusing particles combines to create a fluctuating intensity signal. As the particles continue to diffuse, the intensity will change over time. The speed of these intensity fluctuations depends on the particles' diffusion rate. The smaller the particle, the more rapid the fluctuations, and vice-versa (larger particles have slower fluctuations). Snapshots of the light scattering signal are taken rapidly in sequence, whilst constantly comparing these back to the original signal that was measured. Now, between consecutive snapshots, the intensity signals are similar (or well correlated). However, for snapshots that are further apart in time, the similarity (or correlation) starts to be reduced. Soon, the intensity signal changes completely and there is no longer any correlation with the original measured signal. This process is known as autocorrelation. The larger the particles being measured, the slower the diffusion and the longer it takes for a complete loss of the correlation signal. However, smaller particles have a rapid diffusion, and the correlation of the signal will decay rapidly. Now, auto-correlation enables one to determine the translational diffusion coefficient *D*. Then, one can use the Stokes-Einstein equation to determine the hydrodynamic diameter d_H, in which κ is Boltzmann's constant, T is the absolute temperature, η is the dynamic viscosity, and D is the diffusion coefficient [11]:

$$d_H = \frac{\kappa T}{3\pi\eta D} \quad (1)$$

5.1.4 Incucyte:

The Incucyte instrument is a live-cell imaging and analysis platform that allows for the quantification of cell behavior over time by automatically collecting and analyzing images. This system offers an insight into active biological processes in real-time [12]. As stated earlier, green fluorescent protein (GFP) DNA was used as the nucleic acid in this project. If nanoparticles are successfully

transfected by cells *in vitro*, their Incucyte images will show green area. Through analysis, this green area can be measured in units of length squared per image.

5.1.5 Gel Electrophoresis:

Gel electrophoresis is used as a procedure to separate DNA fragments according to size. DNA samples (or nanoparticle samples that encapsulate DNA) are loaded into the wells located at one end of a gel, and an electric current is applied to pull them through this gel. Since the DNA fragments are negatively charged, they will travel towards the positive electrode. Now, because all the DNA fragments have the same amount of charge per mass, small fragments move through the gel faster than large ones do. A gel is stained with a DNA-binding dye, so the DNA fragments can be seen as bands, each indicating a group of DNA fragments of the same size [13]. In this project, the used gel was 0.8% Agarose (GP). Nanoparticle samples were compared to DNA with buffer at the same concentration as DNA would be inside the nanoparticles. When run through gel electrophoresis, nanoparticle samples that are efficient at encapsulating DNA will show very faint bands, and vice-versa for non-efficient ones, whereas the DNA with a buffer will show the most intense bands.

5.1.6 Inlet Velocity Study:

An inlet velocity study was done for decreasing total flow rates:

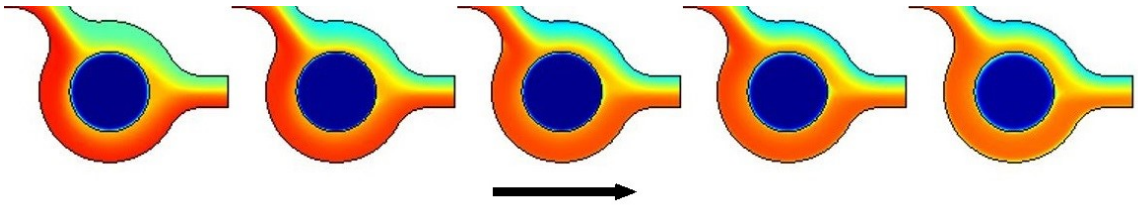

Figure 5.5: Concentration of the nucleic acid solution at the outlet. The total flow rate decreases from left to right. The organic solution's velocity (v_1) starts at 0.1 cm/s and decreases in halves until 0.00625 cm/s. The nucleic acid solution's velocity (v_2) starts at 0.2 cm/s and decreases in halves until 0.0125 cm/s

5.1.7 Velocity Ratio Study:

A velocity of ratio study was done for various velocity ratios:

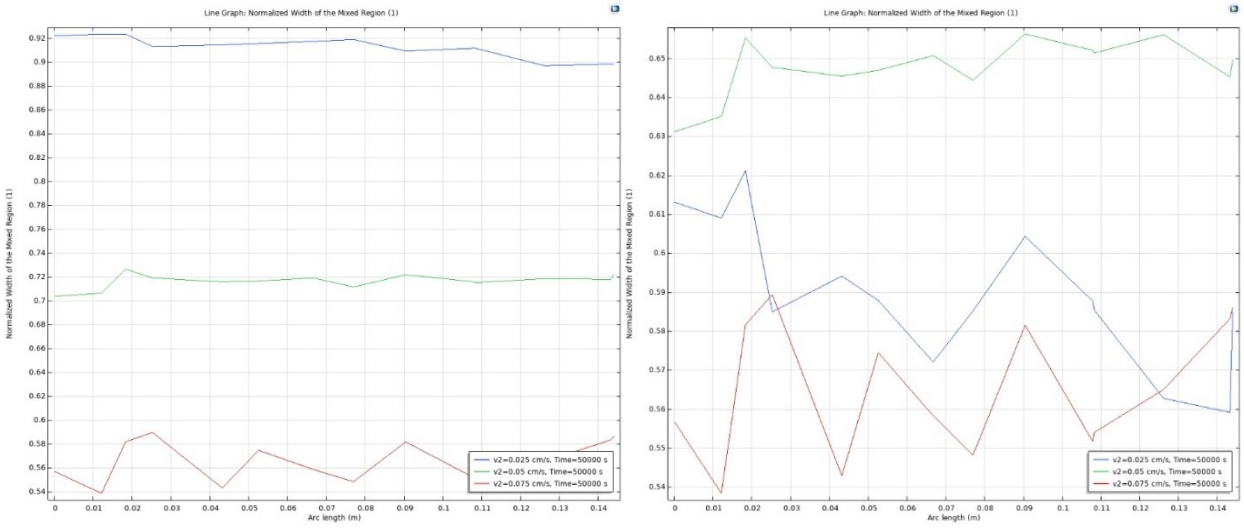

Figures 5.6 & 5.7: Width of the mixed region at the outlet of the mixer for different velocity ratios. (Left, $c_1 = c_2$) (Right, $c_1 = 2c_2$)

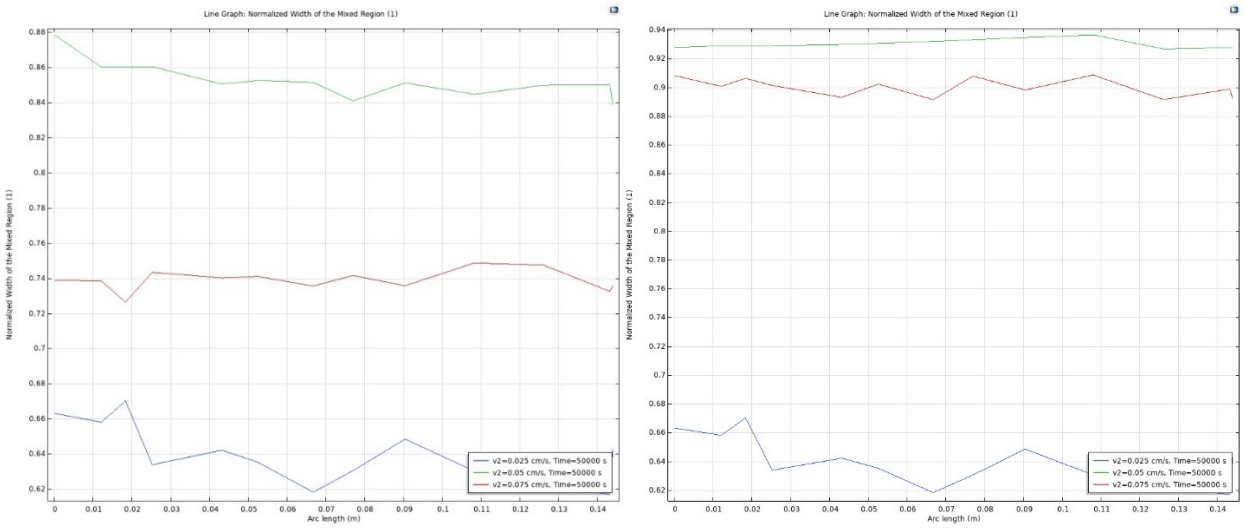

Figures 5.8 & 5.9: Width of the mixed region at the outlet of the mixer for different velocity ratios. (Left, $c_1 = 3c_2$) (Right, $c_1 = 4c_2$)

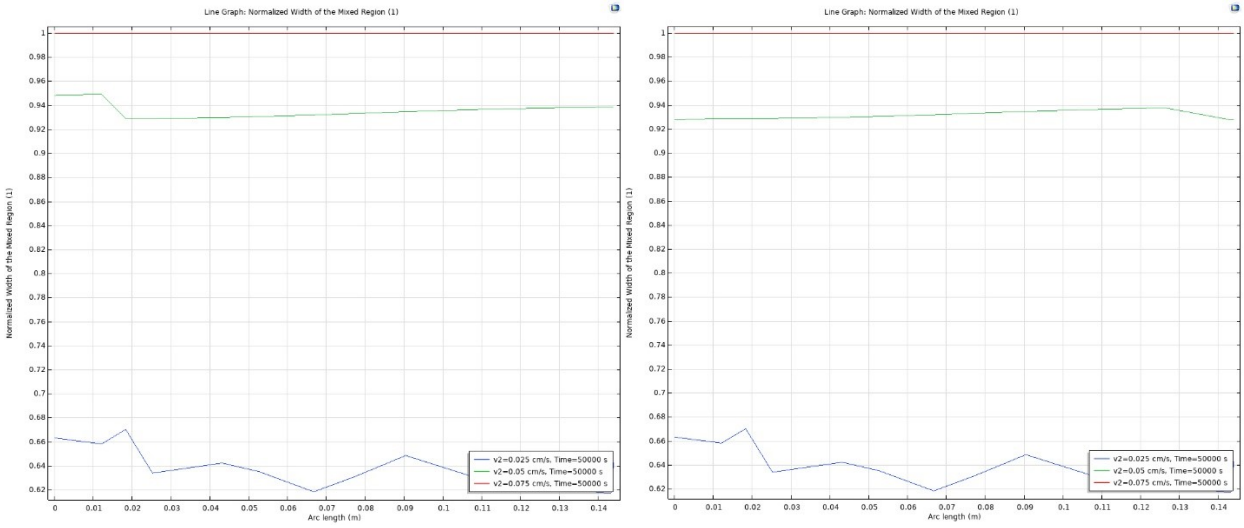

Figures 5.10 & 5.11: Width of the mixed region at the outlet of the mixer for different velocity ratios. (Left, $c_1 = 5c_2$) (Right, $c_1 = 6c_2$)

5.2 Bibliography:

[1] D. M. Loy, P. M. Klein, R. Krzysztoń, U. Lächelt, J. O. Rädler, and E. Wagner, “A microfluidic approach for sequential assembly of siRNA polyplexes with defined structure – activity relationship,” *PeerJ Preprints*, pp. 1–1, Apr. 2019.

[2] C. B. Roces, G. Lou, N. Jain, S. Abraham, A. Thomas, G. W. Halbert, and Y. Perrie, “Manufacturing considerations for the development of lipid nanoparticles using Microfluidics,” *Pharmaceutics*, vol. 12, no. 11, pp. 1–12, Nov. 2020.

[3] K. Ward and Z. H. Fan, “Mixing in microfluidic devices and enhancement methods,” *Journal of Micromechanics and Microengineering*, vol. 25, no. 9, pp. 1–1, Aug. 2015.

[4] Precision NanoSystems, *NanoAssemblr® Spark™ User Guide*. 2021.

[5] X. Hou, T. Zaks, R. Langer, and Y. Dong, “Lipid nanoparticles for mRNA delivery,” *Nature Reviews Materials*, vol. 6, no. 12, pp. 1086–1086, Dec. 2021.

[6] “Lipid nanoparticle resources,” *Lipid Nanoparticles*. [Online]. Available: https://www.precisionnanosystems.com/workflows/formulations/lipid-nanoparticles. [Accessed: 04-Mar-2022].

[7] “Resource center,” *NxGen - A Disruptive Technology Enabling Transformative Medicine*. [Online]. Available: https://www.precisionnanosystems.com/platform-technologies/nxgen. [Accessed: 07-Nov-2021].

[8] “Jann5s/Measuretool,” *MathWorks*. [Online]. Available: https://www.mathworks.com/matlabcentral/fileexchange/25964-jann5s-measuretool#:~:text=Measure%20Tool%20is%20a%20matlab,to%20aid%20measurements%20on%20images.&text=The%20main%20motivation%20behind%20the,image%20magnification%20changes%20while%20measuring. [Accessed: 25-Sep-2021].

[9] “The Transport of Diluted Species Interface,” *COMSOL Documentation*. [Online]. Available: https://doc.comsol.com/5.6/doc/com.comsol.help.chem/chem_ug_chemsptrans.08.049.html#:~:text=The%20Transport%20of%20Diluted%20Species%20(tds)%20interface%20(%20)%2C,be%20handled%20with%20this%20interface. [Accessed: 15-Jan-2022].

[10] *Microchannel Mixing in COMSOL*. BME306 purdue, 2021.

[11] *Introduction to Dynamic Light Scattering Analysis*. Malvern Panalytical, 2019.

[12] “Incucyte® Live-Cell Analysis System, Software, Reagents & Consumables,” *Incucyte® Products | Live-Cell Imaging, Analysis and Reagents*. [Online]. Available: https://www.essenbioscience.com/en/products/. [Accessed: 22-Apr-2022].

[13] “Gel electrophoresis (article),” *Khan Academy*. [Online]. Available: https://www.khanacademy.org/science/ap-biology/gene-expression-and-regulation/biotechnology/a/gel-electrophoresis#:~:text=Gel%20electrophoresis%20is%20a%20technique,move%20towards%20the%20positive%20electrode. [Accessed: 22-Apr-2022].